Kinetics and Mechanisms of Hydrolysis of 1,4-Benzodiazepines II: Oxazepam and Diazepam

WESLEY W. HAN ˣ, GERALD J. YAKATAN, and DALE D. MANESS

Abstract □ The hydrolysis kinetics of oxazepam and diazepam leading to a benzophenone product and a glycine derivative were quantified from pH 1 to 11. For oxazepam, two intermediates were isolated and identified, indicating a parallel consecutive reaction mechanism. The hydrolysis occurred uncatalyzed and demonstrated acid–base catalysis for both reaction steps. One intermediate was observed by TLC for diazepam hydrolysis. This intermediate, resulting from breakage of the azomethine linkage, was different than the major intermediate isolated for oxazepam hydrolytic degradation (amide hydrolysis preferred). Stability parameters involving rate constant–temperature dependence are reported.

Keyphrases □ Oxazepam—kinetics and mechanism of hydrolysis, effect of pH □ Diazepam—kinetics and mechanism of hydrolysis, effect of pH □ Hydrolysis—oxazepam and diazepam, kinetics and mechanism, effect of pH □ 1,4-Benzodiazepines—oxazepam and diazepam, kinetics and mechanism of hydrolysis, effect of pH

In a previous report (1), the kinetics and mechanisms of hydrolysis of chlordiazepoxide and demoxepam, 1,4-benzodiazepines of therapeutic interest, were quantitatively described. Chlordiazepoxide undergoes facile transformation to demoxepam by hydrolysis of the methylamino substituent in the 2-position. Subsequently, the 1,4-benzodiazepine nucleus is lost by hydrolysis of the 1,2- and 4,5-bonds, leading to the final products: 2-amino-5-chlorobenzophenone and a glycine derivative.

Although the kinetic and TLC data indicated a parallel consecutive reaction mechanism (*i.e.*, either 1,2- or 4,5-bond hydrolysis may initially occur), complete data analysis showed that initial azomethine hydrolysis was relatively unimportant to the overall hydrolysis kinetics. An investigation of kinetics and mechanisms of hydrolysis of oxazepam (I*a*) and diazepam (I*b*) was initiated to delineate structural effects on the relative importance of the two mechanistic paths leading to the final products.

EXPERIMENTAL

Materials—TLC was used to verify the purity of oxazepam[1], 2-amino-5-chlorobenzophenone[1], and diazepam[2]. These compounds were chromatographically pure and were used as received. All other chemicals were reagent grade quality. Aqueous solutions were prepared using distilled deionized water. All aqueous solutions were buffered using the following systems: hydrochloric acid, acetate, phosphate, borate, and sodium hydroxide.

Kinetic Measurements and Compound Identification—Hydrolysis kinetics were followed spectrophotometrically. Detailed procedures describing the kinetic measurements and methods used in isolation and identification were reported previously (1). TLC analysis of hydrolytic reaction solutions of diazepam was identical to that used for chlordiazepoxide (1).

For oxazepam, samples of about 10^{-3} *M* solution were withdrawn at appropriate times. These samples were extracted three times with an equal volume of chloroform. A UV scan of the aqueous phase indicated that extraction was complete. The chloroform extract was concentrated and subjected to TLC analysis, using 250-μm silica gel GF plates and chloroform–toluene–methanol (52:48:7) as the developing solvent.

[1] Wyeth Laboratories, Philadelphia, Pa.
[2] Hoffmann-La Roche Inc., Nutley, N.J.

RESULTS AND DISCUSSION

Scheme I gives the general expected mechanism if concomitant 1,2-amide and 4,5-azomethine hydrolyses occur. Compound II would result from 1,2-amide hydrolysis; III is the intermediate derived from hydrolysis of the 4,5-azomethine bond; and IV represents the final products, the substituted benzophenone and the glycine derivative. The initial parallel reaction steps may be reversible under appropriate conditions (1, 2) and are shown. A mathematical treatment of this scheme according to differential absorbance measurements may be found in a prior report (1).

Spectral Changes and Rate Constant Determinations—Two pKa's, 1.7 and 11.6, have been reported for oxazepam at 25° (3). The lower value is attributable to protonation of the azomethine nitrogen, and the larger one is due to deprotonation of the amide nitrogen. Since the proposed intermediates and products are also subject to prototropic reactions, it is not surprising that the kinetic spectra are influenced by pH changes. Throughout the entire pH region, two apparent reaction steps were spectrally observed for oxazepam. Typical spectral changes, demonstrating a two-step reaction, are shown in Fig. 1. The final spectrum is identical to that of 2-amino-5-chlorobenzophenone.

For oxazepam, time plots of the logarithm of differential absorbance measurements at any time and time infinity ($A_t - A_\infty$) consisted of two linear segments according to the biexponential equation:

$$A_t - A_\infty = M \exp(-b_1 t) + N \exp(-b_2 t) \qquad \text{(Eq. 1)}$$

where M and N are preexponential constants and b_1 and b_2 are exponential factors related to the observed rate constants of the first-order reactions in Scheme I. Typical apparent first-order plots are given in Figs. 2 and 3. Feathering was employed to differentiate the two linear seg-

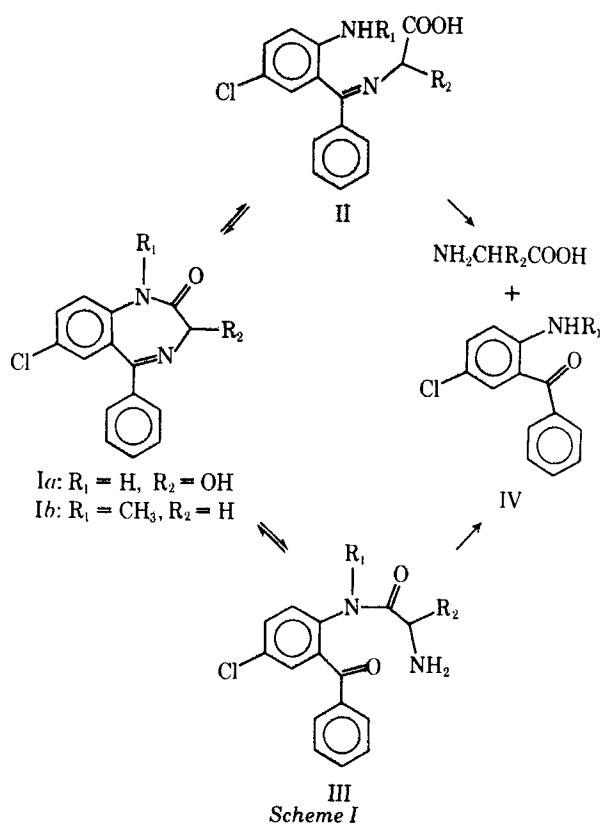

Scheme I

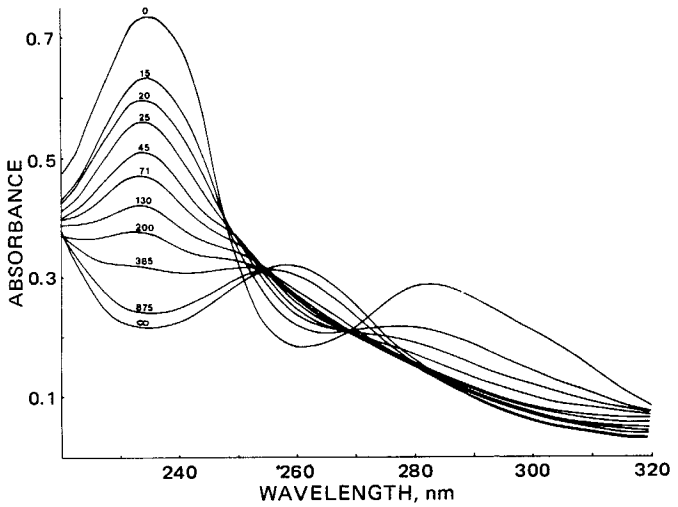

Figure 1—*Typical spectral changes for the hydrolysis of 10^{-5} M oxazepam in 0.1 N HCL, μ = 1.0, at 80°. Curves are labeled as to minutes after initiation of the reaction.*

ments. The apparent first-order rate constants, calculated by least-squares fitting, are reported in Table I.

Diazepam differs from oxazepam in that only one pKa has been observed in the normal pH region (3). The pKa of 3.3 is reportedly due to protonation at the azomethine nitrogen in the 4-position. Due to the methyl substitution on the amide nitrogen, the higher pKa observed with oxazepam, attributable to deprotonation of the amide proton, is absent. At pH values below the pKa of diazepam, observed spectral changes indicated an apparent two-step reaction, both being first order. Above this pKa, spectra of sequential samples demonstrated clear isosbestic points, implicating a single reaction step in a one-to-one kinetic transformation of diazepam to 2-methylamino-5-chlorobenzophenone. Throughout the pH region, the final spectrum was superimposable on that of an equimolar solution of this product.

Below the pKa of diazepam, the apparent rate constants were calculated by the same procedure as used for oxazepam. In the pH region showing a single reaction step, the observed rate constants were determined according to the integrated first-order expression:

$$\ln(A_t - A_\infty) = \ln(A_0 - A_\infty) - kt \qquad \text{(Eq. 2)}$$

Linear segments for both the biexponential and monoexponential plots were clearly first order, as indicated by the correlation coefficients, r, in Tables I and II. The least-squares estimates of the rate constants for diazepam are given in Table II.

Rate–pH Profiles—The log k–pH profile for oxazepam hydrolysis (Fig. 4) was generated from the rate constants given in Table I. The two reaction steps are shown on the same log k–pH profile: the initial step, hydrolysis of oxazepam to an intermediate(s), and the second, slower reaction representing hydrolysis of the intermediate(s) to the final products. For the initial hydrolytic step, the equation that defines the

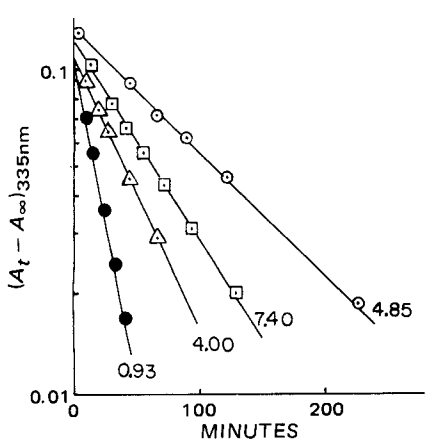

Figure 2—*Typical apparent first-order plots for the first hydrolytic reaction step of oxazepam at 85°, μ = 1.0. Feathered lines are labeled as to pH values.*

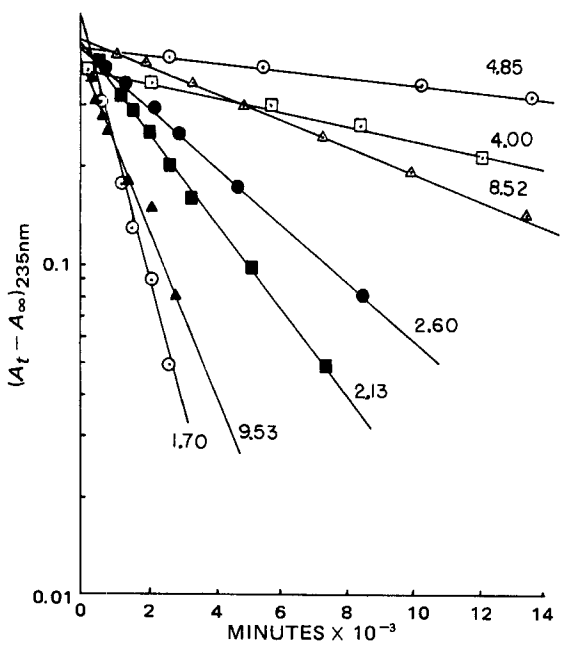

Figure 3—*Typical apparent first-order plots for the second hydrolytic reaction step of oxazepam at 85°, μ = 1.0. Lines are labeled as to pH values.*

theoretical curve drawn through the experimental points is:

$$k_{obs} = k_H[H^+]f_{H_2S} + k_{H'}[H^+]f_{HS} + k'_{H_2O}f_{HS} + k_{OH'}[OH^-]f_{HS} + k_{OH''}[OH^-]f_S \qquad \text{(Eq. 3)}$$

where the observed rate constant (k_{obs}) is defined as a function of the specific bimolecular rate constants (k_H, k_{H_2O}, and k_{OH}), the specific catalyzing species (H^+ and OH^-), and the fractions of diprotic (f_{H_2S}), monoprotic or uncharged (f_{HS}), and deprotonated oxazepam (f_S), respectively. This general equation may be substituted with the following

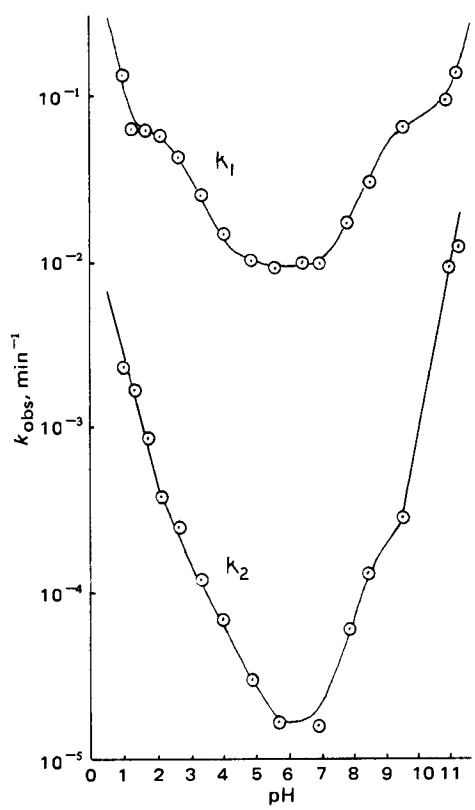

Figure 4—*Log k–pH profile for the hydrolysis of oxazepam at 85°, μ = 1.0.*

Table I—Apparent First-Order Rate Constants, 10^4 k (in Minutes^{-1}) for Oxazepam at 85°, μ = 1.0

pH	Buffer, M		k_1[a]	k_2[a]	r_1	r_2
		[HCl]				
0.93		0.1000	1324.9 ± 280.2	24.42 ± 4.01	0.93	0.93
1.24		0.0398	669.0 ± 128.5	16.95 ± 0.08	0.96	0.99
1.70		0.0158	633.9 ± 62.98	8.66 ± 0.20	0.99	0.99
2.13		0.0063	589.6 ± 79.6	3.84 ± 0.11	0.97	0.99
2.60		0.0025	436.5 ± 49.8	2.50 ± 0.08	0.97	0.99
	[CH_3COOH]	[CH_3COO^-]				
3.24	0.0957	0.0043	254.2 ± 9.2	1.18 ± 0.11	0.99	0.98
4.00	0.0761	0.0239	151.0 ± 6.2	0.68 ± 0.03	0.99	0.99
4.85	0.0322	0.0678	102.1 ± 1.1	0.28 ± 0.01	0.99	0.99
	[$H_2PO_4^-$]	[HPO_4^{2-}]				
5.58	0.0553	0.0011	92.9 ± 1.7	0.16 ± 0.008	0.99	0.99
6.47	0.0275	0.0391	103.1 ± 2.1	0.29 ± 0.008	0.99	0.99
	[H_3BO_3]	[$H_2BO_3^-$]				
6.96	0.103	0.003	100.8 ± 10.3	0.15 ± 0.02	0.97	0.98
7.93	0.103	0.029	177.9 ± 1.8	0.59 ± 0.05	0.99	0.98
8.52	0.061	0.112	331.1 ± 4.8	1.33 ± 0.11	0.99	0.99
9.53	0.003	0.100	628.8 ± 160.0	2.87 ± 1.33	0.94	0.77
		[NaOH]				
10.90		0.05	980.8 ± 18.3	95.54 ± 27.83	0.99	0.77
11.23		0.10	1421.9 ± 55.7	126.75 ± 1.15	0.99	0.99

[a] Standard deviations were calculated from a linear regression analysis of the data.

kinetic equivalents:

$$k_{H_2O}f_{H_2S} = k_{H'}[H^+]f_{HS} \quad \text{(Eq. 4)}$$

$$k_{OH}[OH^-]f_{H_2S} = k'_{H_2O}f_{HS} \quad \text{(Eq. 5)}$$

$$k_{OH'}[OH^-]f_{HS} = k''_{H_2O}f_S \quad \text{(Eq. 6)}$$

The respective fractions may also be written in terms of proton concentration and the acidity constants of oxazepam, K_1 and K_2, as, for example:

$$f_{H_2S} = \frac{[H^+]^2}{[H^+]^2 + K_1[H^+] + K_1K_2} \quad \text{(Eq. 7)}$$

The bimolecular rate constants and kinetic pKa's that provided the optimal fit to the experimental data points are listed in Table III. The calculated pKa's, 3.0 and 8.8, deviated substantially from those previously given as 1.7 and 11.6 at 25°. This deviation is reconcilable with the temperature difference between 85° (kinetic determination) and 25° (literature value). The directions of the shifts would be expected from thermodynamic consideration of the charged species in the protropic reactions.

The log k–pH profile for the second reaction step mirrors that of the initial step, and Eq. 3 may be used to generate the theoretical curve through the experimental data points. However, the fractions present (f_{H_2S}, f_{HS}, and f_S) would in this case refer to the intermediate(s), as would the kinetic pKa's. The theoretical curve was constructed from the values of the bimolecular rate constants and pKa values given in Table III.

The log k–pH profile for diazepam is given in Fig. 5. For pH values below the pKa of diazepam, two reaction steps were observed. The first reaction step is quantitatively described by the expression:

$$k_{obs} = k_{H_2O}f_{HS} \quad \text{(Eq. 8)}$$

or by its kinetic equivalent:

$$k_{obs} = k_H[H^+]f_S \quad \text{(Eq. 9)}$$

The kinetic pKa was determined to be 2.9, compared to the value of 3.3 at 25°. The magnitude and direction of the change in the pKa do not agree with those observed for the lower pKa value of oxazepam, both involving deprotonation of the azomethine nitrogen. The reason for this difference is not apparent. The second reaction step, as well as the single reaction step at higher pH values, is attributable to hydrolysis of a reaction intermediate according to the expression:

$$k_{obs} = k_H[H^+]f_{HS} + k_{H'}[H^+]f_S + k_{OH}[OH^-]f_S \quad \text{(Eq. 10)}$$

The second term, involving acid catalysis of the deprotonated intermediate, is kinetically equivalent to uncatalyzed hydrolysis of the protonated form. Table III lists the bimolecular rate constants and pKa values used to generate the theoretical curve shown in Fig. 5.

Isolation and Identification—Oxazepam samples withdrawn at appropriate times were subjected to TLC analysis as previously described. Throughout the entire pH region, the oxazepam spot (R_f 0.23) showed a gradual decrease in intensity with a concomitant relative intensity increase for that of the product 2-amino-5-chlorobenzophenone (R_f 0.75). The glycine derivative was observed at the origin upon spraying with

Table II—Apparent First-Order Rate Constants, 10^4 k (in Minutes^{-1}) for Diazepam at 80°, μ = 1.0

pH	Buffer, M		k_1[a]	k_2[a]	r_1	r_2
		[HCl]				
0.93		0.1000	940 ± 188	5.30 ± 0.11	0.97	0.99
1.70		0.0158	562 ± 104	1.71 ± 0.04	0.98	0.99
2.60		0.0025	640 ± 100	0.56 ± 0.07	0.90	0.97
	[CH_3COOH]	[CH_3COO^-]				
3.24	0.0957	0.0043	279 ± 6.15	0.26 ± 0.03	0.99	0.97
4.00	0.0761	0.0239	—	<0.10	—	—
4.85	0.0322	0.0678	—	<0.10	—	—
5.64	0.0081	0.0919	—	<0.10	—	—
	[$H_2PO_4^-$]	[HPO_4^{2-}]				
5.58	0.0553	0.0011	—	<0.10	—	—
6.47	0.0275	0.0391	—	<0.10	—	—
	[H_3BO_3]	[$H_2BO_3^-$]				
6.96	0.103	0.003	—	<0.10	—	—
7.93	0.103	0.029	—	<0.10	—	—
8.52	0.061	0.112	0.18 ± 0.01	—	0.99	—
9.63	0.003	0.100	0.57 ± 0.01	—	0.99	—
		[NaOH]				
10.18		0.01	1.75 ± 0.77	—	0.99	—
10.90		0.05	26.10 ± 0.77	—	0.99	—

[a] Standard deviations were calculated from a linear regression analysis of the data.

Table III—Bimolecular Rate Constants[a] for Hydrolysis of Oxazepam and Diazepam, μ = 1.0

k_H	k_H'	k_{H_2O}	k'_{H_2O}	k''_{H_2O}	k_{OH}	k_{OH}'	k_{OH}''	pKa[b]
				Oxazepam, k_1, 85°				
1.0	65	0.065	0.0098	0.072	4.18×10^7	487	2.0	3.0, 8.8
				Oxazepam, k_2, 85°				
0.023	1.44	0.000115	0.000014	0.00012	4070	4.07	0.4	4.1, 8.1
				Diazepam, k_1, 80°				
—	—	—	0.09	—	0.08	—	—	2.9
				Diazepam, k_2, 80°				
0.0045	0.11	—	—	—	—	—	—	3.4

[a] Except that 55.5 M water is incorporated into the k_{H_2O}, the rate constants are in units of minutes^{-1} M^{-1}. [b] The calculated kinetic pKa for the hydrolysis.

ninhydrin aerosol (0.5%). Two additional spots appeared transiently (R_f 0.48 and 0.68) and were ascribed to reaction intermediates. At pH values below pKa, the relative intensities of the intermediate spots appeared similar. However, at higher pH values, the spot at R_f 0.68 was much more intense than that at R_f 0.48.

The intermediates were isolated by preparative TLC and characterized spectroscopically. Structure IIa of Scheme I was assigned to the intermediate (R_f 0.68) predominating at the higher pH values by these measurements. The IR spectrum of a potassium bromide disk showed a typical carbonyl absorption peak at 1725 cm^{-1} for the carboxylic acid functional group. The NMR spectrum taken in dimethyl sulfoxide-d_6 demonstrated an acid proton (τ = −0.2). The expected molecular ion at m/e 304 was not observed in the mass spectrum analysis. The ion of greatest mass was observed at m/e 284. Sadee and Kleijn (4) demonstrated that the thermolysis of oxazepam leads to 6-chloro-4-phenylquinazoline-2-carboxaldehyde in GLC. It is possible that a comparable rearrangement of intermediate IIa, leading to the formation of 6-chloro-4-phenylquinazoline-2-carboxylic acid (mol. wt. 284), occurred in the ionization chamber of the mass spectrometer.

The IR and NMR spectra of the second intermediate were compatible with Structure IIIa of Scheme I but not definitive. The mass spectrum showed a parent peak of m/e 287 instead of the molecular ion of IIIa (m/e 304). Oxazepam, mol. wt. 286, gives a parent peak at m/e 269, indicating that dehydroxylation is a favored fragmentation. A similar preference for IIIa would account for the absence of the 304 peak and the appearance of the 287 peak. Thus, Structure IIIa was tentatively assigned to the intermediate (R_f 0.48).

TLC analysis of the hydrolysis of diazepam indicated formation of one intermediate (R_f 0.58) at pH values below the pKa. Diazepam and the product 2-methylamino-5-chlorobenzophenone were observed at R_f 0.43 and 0.69, respectively. At pH values above the pKa, no spots attributable to reaction intermediates were observed. The product glycine was identified at the origin by spraying with 0.5% ninhydrin aerosol reagent throughout the entire pH region. Attempts to isolate sufficient quantities of the intermediate for identification were unsuccessful due to the small amount present.

If the assumption is made that the intermediate is either IIb or IIIb, then the log k–pH profile may be used to suggest which is the most likely candidate. The discontinuity observed for the first reaction step at pH values above the pKa may be attributable to a recyclization reaction, adding a reversible reaction to the consecutive kinetic scheme. Structure IIb would exist as a protonated amine at pH values below its pKa and in the neutral form above the pKa. No recyclization would be expected with the protonated form due to the expected decreased nucleophilicity. However, the free base form could be expected to undergo facile recyclization. Thus, Structure IIIb was tentatively assigned to the intermediate resulting from diazepam hydrolysis.

Hydrolytic Mechanisms—The mechanisms of hydrolysis for oxazepam and diazepam may be interpreted according to Scheme I. For each, the pKa in the acidic pH region provides a pivotal point. At pH values above this point, II should exist as the carboxylate anion. This charge character would decrease the likelihood of nucleophilic attack of the aromatic amine necessary for reversibility. At lower pH values, the conjugate acid form should be susceptible to recyclization analogous to that observed with chlordiazepoxide (1) and demoxepam (2).

Intermediate III should demonstrate the opposite charge character as a function of pH. At pH values below its pKa, the amine function should be predominately protonated and thus have a resident positive charge. In this form, the nitrogen should be ineffective as a nucleophile, and recyclization would not occur. As the conjugate base above the pKa, reversibility would be much more favorable.

The observation that two intermediates are present during oxazepam hydrolysis implies that the parallel consecutive reaction mechanism shown in Scheme I is operable throughout the entire pH region. At pH values below the pKa, biphasic kinetic behavior was observed. These kinetics would be consistent with the parallel consecutive scheme if the transformation of the intermediates to final products is of approximately equal magnitude. The appearance and loss of the intermediates were qualitatively observed by TLC to be occurring at equal rates. At pH values above the pKa, TLC indicated that IIa formation was preferred. This phenomenon, coupled with the biphasic character of the kinetics, implies that the kinetically relevant mechanism is that shown in Scheme II.

$$Ia \rightarrow IIa \rightarrow IVa$$

Scheme II

Recyclization of intermediate IIIa and the absence of reversible reaction for Ia → IIa kinetically favor this pathway. Models show that sterically amide hydrolysis should be preferential to breakage of the azomethine bond. The competitiveness observed in the lower pH region appears to be attributable to the reversibility differences of the initial,

Table IV—Apparent First-Order Rate Constants, 10^4 k (in Minutes^{-1}) and Thermodynamic Parameters for Hydrolysis of Diazepam and Oxazepam

pH	k_i	85°	80°	75°	70°	E_a[a], kcal/mole	ln P[a]
				Diazepam			
0.93	k_1	157.0	94.0	67.0	49.6	18.4 ± 1.9	24.0 ± 2.8
	k_2	8.46	5.22	3.43	2.06	22.7 ± 0.6	24.7 ± 0.8
10.18	k_1	2.3	1.7	1.2	0.8	17.2 ± 0.6	15.9 ± 0.9
				Oxazepam			
0.93	k_1	1325	806	466	288	24.2 ± 0.5	33.0 ± 0.8
	k_2	24.4	18.6	12.9	10.9	13.5 ± 1.3	13.0 ± 1.9
3.24	k_1	254	208	118	78.1	20.0 ± 2.3	24.6 ± 3.3
	k_2	1.18	0.92	0.63	0.51	12.9 ± 1.1	9.1 ± 1.6
8.52	k_1	331	247	100	74.9	26.1 ± 4.2	33.4 ± 6.0
10.90	k_1	981	757	479	243	22.5 ± 3.0	29.5 ± 4.3
	k_2	95.5	67.1	42.2	21.7	24.0 ± 2.2	29.2 ± 3.1

[a] Standard deviations were calculated from a linear regression analysis of the data.

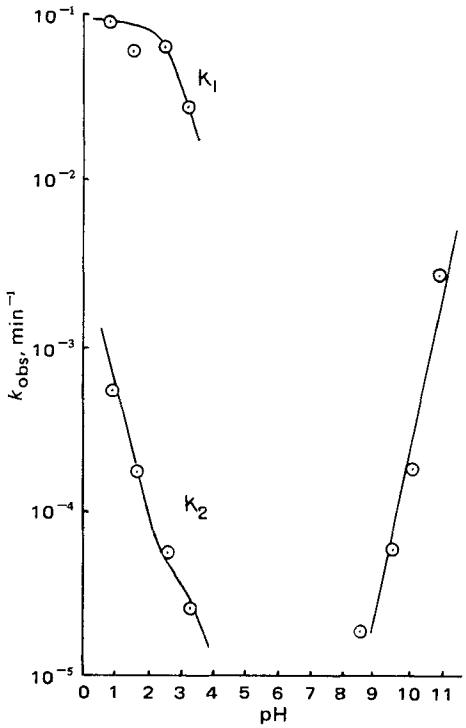

Figure 5—*Log* k–*pH profile for the hydrolysis of diazepam at 80°, μ = 1.0.*

parallel steps. Additionally, the charge character of the intact benzodiazepine, brought about by protonation of the azomethine nitrogen at lower pH values, electronically favors nucleophilic attack on the 5-position.

Diazepam hydrolysis proceeds through one intermediate (Scheme III).

$$Ib \rightarrow IIIb \rightarrow IVb$$

Scheme III

Apparently, methyl substitution on the amide nitrogen makes initial azomethine hydrolysis the preferred pathway. At pH values below the pKa, III*b* is not subject to recyclization; clear biphasic kinetics result. In the higher pH region, facile recyclization of III*b* causes the kinetics to be monophasic in character (Scheme IV).

$$Ib \rightleftharpoons IIIb \rightarrow IVb$$

Scheme IV

The Arrhenius parameters for hydrolysis were obtained from the slope and intercept of a plot of the logarithm of the apparent first-order rate constant, k, *versus* the reciprocal of the absolute temperature, T, shown by the expression:

$$\ln k = \ln P - E_a/RT \qquad \text{(Eq. 11)}$$

where R is the gas constant equal to 1.987 cal deg^{-1} mole^{-1}; $\ln P$ is related to the entropy of activation, ΔS_a, by:

$$\Delta S_a = R[\ln P - \ln(kT/h) - 1] \qquad \text{(Eq. 12)}$$

where h and k are the Planck and Boltzman constants, respectively; and E_a is related to the enthalpy of activation of the hydrolysis, ΔH_a, by:

$$\Delta H_a = E_a - RT \qquad \text{(Eq. 13)}$$

The Arrhenius parameters for oxazepam and diazepam hydrolyses at various pH values are given in Table IV. These values allow stability prediction in the pH regions showing rapid degradation. For oxazepam, buffer catalysis was studied according to the relationship:

$$k_{obs} = k_0 + \left(\frac{k_{HA}[H^+]}{K_a} + k_A\right)[A^-] \qquad \text{(Eq. 14)}$$

where K_a is the dissociation constant for the buffer species; k_0 is the hydrolysis rate constant in the absence of buffer catalysis; and k_{HA} and k_A are the rate constants for buffer catalysis of the acid buffer species, HA, and its conjugate base, A^-, respectively. Buffer effects were investigated by changing the original buffer concentration fourfold in a gradient manner. Buffer effects were not significant, and thus the specific rate constants were not delineated.

REFERENCES

(1) W. W. Han, G. J. Yakatan, and D. D. Maness, *J. Pharm. Sci.*, **65,** 1198 (1976).

(2) L. H. Sternback and E. Reeder, *J. Org. Chem.*, **26,** 4936 (1961).

(3) J. Barrett, W. F. Smyth, and I. E. Davidson, *J. Pharm. Pharmacol.*, **25,** 387 (1973).

(4) W. Sadee and V. D. Kleijn, *J. Pharm. Sci.*, **60,** 135 (1971).

ACKNOWLEDGMENTS AND ADDRESSES

Received November 28, 1975, from the *College of Pharmacy, University of Texas at Austin, Austin, TX 78712.*

Accepted for publication June 15, 1976.

Presented in part at the Basic Pharmaceutics Section, APhA Academy of Pharmaceutical Sciences, San Francisco meeting, April 1975.

Abstracted in part from a dissertation submitted by W. W. Han to the University of Texas at Austin in partial fulfillment of the Doctor of Philosophy degree requirements.

Supported in part by a grant from the University Research Institute, University of Texas at Austin.

The authors express their gratitude to Dr. W. E. Scott, Hoffmann–La Roche Inc., and to Dr. G. Schneller, Wyeth Laboratories, for samples supplied and to Dr. Jay Nematollahi for helpful discussions.

[x] To whom inquiries should be directed. Present address: Searle Laboratories, Chicago, IL 60680.